

## ChemComm

## Li<sub>2</sub>NbHO<sub>2</sub>: a new transition-metal oxyhydride with rocksalt-type structure

Journal:	ChemComm			
Manuscript ID	CC-COM-10-2024-005503.R1			
Article Type:	Communication			

SCHOLARONE™ Manuscripts

### **COMMUNICATION**

# Li<sub>2</sub>NbHO<sub>2</sub>: a new transition-metal oxyhydride with rock-salt-type structure

Fumitaka Takeiri,<sup>a,b</sup> Keiko Kusumoto,<sup>a,c</sup> Kosuke Kawai,<sup>d</sup> Hiroshi Yaguchi,<sup>a</sup> Takashi Saito,<sup>e</sup> Kazuhiro Mori,<sup>e</sup> Saburo Hosokawa,<sup>f</sup> Masashi Okubo,<sup>d</sup> Genki Kobayashi\*<sup>a,d</sup>

Received 00th January 20xx, Accepted 00th January 20xx

DOI: 10.1039/x0xx00000x

Transition-metal oxyhydrides are an emerging class of functional materials; however, the known compounds have mostly been limited to perovskite-type sturctures. Here, we successfully synthesized  $\text{Li}_2\text{NbHO}_2$ , the first example of a rock-salt-type transition-metal oxyhydride, using mechanochemical methods. Galvanostatic charge/discharge tests revealed that  $\text{Li}_2\text{NbHO}_2$  functions as an electrode for lithium secondary batteries.

Mixed anion oxides containing hydride ions (H<sup>-</sup>), known as hydride-oxides or oxyhydrides, are an emerging class of functional inorganic solids. For example, BaTiO<sub>3-x</sub>H<sub>x</sub><sup>1, 2</sup> and BaCe(O,H,N)<sub>3</sub><sup>3</sup> exhibit high catalytic activity for hydrogenation reaction, while  $A_2$ Li(H,O)<sub>4-\delta</sub> (A = La, Sr, Ba)<sup>4, 5</sup> and LaH<sub>3-x</sub>O<sub>x/2</sub><sup>6</sup> enable fast H<sup>-</sup> conduction. Moreover, some fundamentally interesting phenomena occur when H<sup>-</sup> ions coexist with transition-metal (TM) ions (d-electrons). The absence of  $\pi$  symmetry in the H<sup>-</sup> valence shell (1s orbital) critically affects the interactions in one-dimensional TM-H-TM chains; e.g. in SrVO<sub>2</sub>H, V  $t_{2g}$  H 1s orbitals are much weaker than V-O-V interactions due to the orbital orthogonality<sup>7</sup>. A theoretical study of hydrogen configuration introduced into SrTiO<sub>3</sub> suggests that the zwitterionic nature of hydrogen could enable electron transfer to/from the Ti ion (H<sup>-</sup>  $\leftrightarrow$  2e<sup>-</sup> + H<sup>+</sup>)<sup>8</sup>.

<sup>a.</sup> Solid State Chemistry Laboratory, Cluster for Pioneering Research (CPR), RIKEN, Saitama 351-0198, Japan

E-mail: genki.kobayashi@riken.jp

However, TM oxyhydrides have so far been limited in terms of structural diversity. In fact, reported compounds are mostly categorized as perovskite and related structures. e.g. simple cubic-type  $ATiO_{3-x}H_x$  (A = Ca, Sr, Ba) $^9$  and  $SrCrO_2H^{10}$ , hexagonaltype  $BaMO_{3-x}H_x$  ( $M = Ti^2$ ,  $V^{11}$ ,  $Cr^{12}$ ), and layered-type LaSrCoO<sub>3</sub>H<sub>0.7</sub><sup>13</sup> and Sr<sub>n+1</sub>V<sub>n</sub>O<sub>2n+1</sub>H<sub>n</sub> (n = 1, 2,  $\infty$ )<sup>14</sup>. Here, we focus on the role of non-TM ions. In "hydrides" composed solely of transition-metals, including TiHx, NiHx, and PdHx, hydrogen typically dissolves in the metal or alloy to form an interstitial solid solution, where hydrogen behaves more like atomic hydrogen (H<sup>0</sup>) rather than as a hydride ion (H<sup>-</sup>). Given that H<sup>-</sup> ions occupy the anionic sites in the above-mentioned oxyhydrides, electropositive (i.e. strongly electron donating) alkaline earth or rare-earth cations should play a critical role in stabilizing H- in the lattice. The relatively large ionic radii of those cations, e.g.  $La^{3+}$  (1.36 Å; CN = 12),  $Sr^{2+}$  (1.44 Å; CN = 12), and  $Ba^{2+}$  (1.61 Å; CN = 12)<sup>15</sup>, may contribute to the formation of perovskite structures; in other words, the Goldschmidt tolerance factor approaches unity. Based on this expectation, the use of smaller electropositive cations like Li<sup>+</sup> and Mg<sup>2+</sup> could enable the preparation of new TM oxyhydrides with other crystal structures such as rock-salt, ilmenite, and LiNbO<sub>3</sub>-types. In this communication, we report the successful synthesis of Li<sub>2</sub>NbHO<sub>2</sub> that is the first example of rock-salt-type TM oxyhydride.

A polycrystalline sample of  $Li_2NbHO_2$  was synthesized using a mechanochemical method that was recently found to be effective for transition-metal oxyhydride synthesis  $^{16}$ . The raw materials LiH (Alfa Aesar, 99.4%),  $Li_2O$  (KOJUNDO, 99%), NbO (KOJUNDO), NbO $_2$  (KOJUNDO, 99.9%) were weighed in a molar ratio of 2:1:1:1, and the mixture was sealed in a 20 mL zirconia pot with 65 zirconia balls with a diameter of 5 mm. High energy ball milling at 800 rpm was conducted using a planetary ball mill apparatus (PL-7, Fritsch). The black powder obtained after milling for 36 hours can be indexed in X-ray diffraction (XRD) as a cubic unit cell with a lattice constant of approximately 4.2 Å in a single phase (Fig. S1†). To

<sup>&</sup>lt;sup>b.</sup> Department of Chemistry, Kindai University, Osaka 577-8502, Japan

<sup>&</sup>lt;sup>c</sup> Department of Structural Molecular Science, School of Physical Sciences SOKENDAI (The Graduate University for Advanced Studies), Aichi 444–8585, Japan

d. Department of Chemistry, Electrical Engineering and Bioscience, Waseda University, Tokyo 169-8555, Japan

Institute of Materials Structure Science, High Energy Accelerator Research Organization (KEK), Ibaraki 305-0801, Japan

f. Faculty of Materials Science and Engineering, Kyoto Institute of Technology, Kyoto 6068585, Japan

<sup>†</sup> Footnotes relating to the title and/or authors should appear here. Electronic Supplementary Information (ESI) available: [details of any supplementary information available should be included here]. See DOI: 10.1039/x0xx00000x

COMMUNICATION Journal Name

avoid unexpected moisture contamination, the powder sample was always handled in an Ar-filled glove box.

Structural information, particularly the presence of H<sup>-</sup> ions in the crystal lattice, was clarified by time-of-flight powder neutron diffraction (ND) experiments. We initially measured the aforementioned product; however, the low signal-to-noise (S/N) ratio due to the incoherent scattering of hydrogen made refinement difficult. Subsequently, we prepared a deuteride product by using LiD instead of LiH as a raw material. Figure 1 shows the Rietveld refinement profile of ND data for the deuteride product, which also consisted of a single cubic unit cell, collected at room temperature. We refined the profile using a structure model with a disordered rock-salt-type structure (space group Fm-3m), where Li/Nb atoms were placed at the Wyckoff position 4b (0, 0, 0) and D/O at 4b (1/2, 1/2, 1/2). Prior to refinement, the Li/Nb ratio of 2.09:1, which is close to the nominal ratio of 2:1, was confirmed by elemental analyses (AAS for Li and ICP-OES for Nb performed by Toray Research Center, Inc.). The refinement converged reasonably with agreement indices of  $R_{wp}$  = 5.36% and  $R_p$  = 4.85%; the parameters are summarized in Table 1.

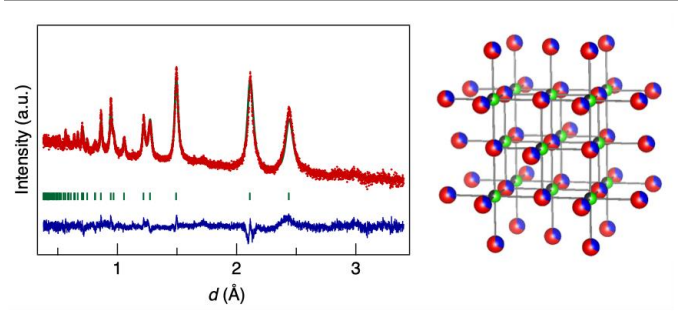


Figure. 1. (left) Powder ND data of Li<sub>2</sub>NbDO<sub>2</sub> collected at room temperature using the SPICA diffractometer at J-PARC. The sample (approximately 0.5 g) was loaded into a cylindrical vanadium cell. Refinement was performed by the Rietveld method using the Z-Rietveld program<sup>17</sup>. The red crosses and green solid curves represent observed and calculated intensities, respectively. The blue solid lines at the bottom indicate residual curves. The green ticks indicate the peak positions of Li<sub>2</sub>NbDO<sub>2</sub>, (right) The crystal structure of Li<sub>2</sub>NbDO<sub>2</sub>, illustrated using the VESTA program<sup>18</sup>. Green, black, blue, and red balls represent Li, Nb, D, and O atoms, respectively.

Table 1. Crystallographic parameters of  $\mathrm{Li_2NbDO_2}$  obtained from Rietveld refinement.

Atom	Site	g	x	у	Z	$B_{\rm iso}$ (Å <sup>2</sup> )
Li	4a	0.6081(9)	0	0	0	0.499(12)
Nb	4a	0.3919(9)	0	0	0	0.499(12)
D	4b	0.33	0.5	0.5	0.5	0.499(12)
0	4b	0.67	0.5	0.5	0.5	0.499(12)

Space group:  $Fm\overline{3}m$  (225); a = 4.21998(16) Å;  $R_{wp} = 5.36\%$ ,  $R_p = 4.85\%$ ,  $R_B = 8.24\%$ ,  $R_F = 3.42\%$ .

Figure 2a shows room-temperature Nb K-edge XANES spectra for the product (black line), along with commercially available Nb<sup>II</sup>O (blue), Nb<sup>IV</sup>O<sub>2</sub> (green), and Nb<sup>V</sup><sub>2</sub>O<sub>5</sub> (red) as references. The absorption edge is located between those of NbO and NbO<sub>2</sub>, suggesting the presence of trivalent Nb in our compound. The absence of protons (hydroxyl groups) in the product was confirmed by Fourier-transform infrared (FT-IR) measurement, as shown in Fig 2b. No sharp peak was observed around 3700 cm<sup>-1</sup>, which contrasts with the stretching vibrations of O–H bonds in the reference LiOH. Based on these

results, along with the electrical neutrality condition, we conclude that the product is a disordered (simple) rock-salt-type oxyhydride, close to the nominal composition of  $\text{Li}_2\text{NbHO}_2$ , although the Li/Nb O/D ratios may contain errors of less than 10%. In addition, thermogravimetric measurements and subsequent XRD results revealed that the compound is stable in Ar and dry O2 atmosphere up to 400 °C and 125 °C, respectively (Fig. S2 and S3†).

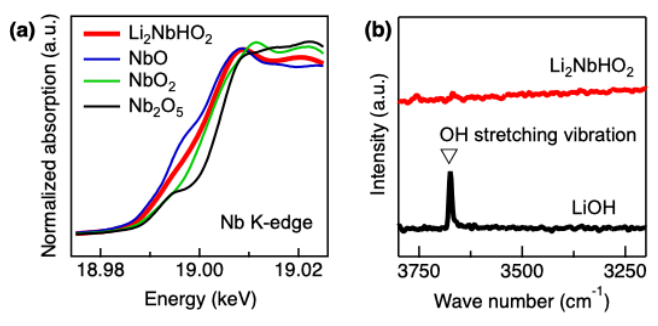


Figure 2 (a) Nb K-edge spectra of  $\text{Li}_2\text{NbHO}_2$  (red) and the reference niobium oxides. The data were collected at room temperature using the beamline BL01B1 of the SPring-8. (b) FT-IR spectra of  $\text{Li}_2\text{NbHO}_2$  (red) and reference LiOH (black) acquired in an Ar-filled glovebox at room temperature. A sharp peak in the LiOH spectrum at ~3700 cm<sup>-1</sup> corresponds to the stretching vibrations of the O–H bonds.

The newly obtained Li<sub>2</sub>NbHO<sub>2</sub> is the first example of a rocksalt-type TM oxyhydride. The discovery of a new class of compounds with such a fundamental crystal structure is notable and somewhat surprising. We believe that many more rock-salttype oxyhydrides of (Li,TM)(H,O) with various Li/TM and H/O ratios, will be found in the future. Moreover, rock-salt type structure has a rich variety of related including layered ones (e.g. α-NaFeO<sub>2</sub>-type), CdCl<sub>2</sub>-type, and spinel-type. Those structures are expected to appear also in oxyhydrides, potentially providing new functions. Note that the synthetic process using high-energy ball-milling could contribute to the successful preparation of Li<sub>2</sub>NbHO<sub>2</sub>. Chemical reactions driven by mechanical energy rather than thermal energy sometimes result in metastable phase<sup>19</sup>. The feature that solid-state reaction proceeds at around room temperature is particularly advantageous for synthesizing hydride-based compounds, that tend to release hydrogen gas (H<sub>2</sub>) when heated.

The discovery of disordered rock-salt-type oxyhydrides is also interesting in terms of electrode material for lithium batteries, especially in relation to lithium-rich oxides and oxyfluorides represented by Li<sub>3</sub>NbO<sub>4</sub><sup>20</sup> and Li<sub>2</sub>Mn<sub>2/3</sub>Nb<sub>1/3</sub>O<sub>2</sub>F<sup>21</sup> for cathode, and by Li<sub>3</sub>V<sub>2</sub>O<sub>5</sub><sup>22</sup> for anode. Here, we performed galvanostatic charge/discharge tests over the voltage range from 1.0 to 4.0 V (vs. Li/Li<sup>+</sup>) at 25 °C using 2032-type coin cells to evaluate the electrode performance of Li<sub>2</sub>NbHO<sub>2</sub>. The current density was set as 38.3 mA g<sup>-1</sup>, that corresponds to C/10 rate, where the theoretical capacity is calculated based on two Li<sup>+</sup> removal per formula unit (383 mA h g<sup>-1</sup>).

Figure 3 shows the charge/discharge curves of  $Li_2NbHO_2$ . Although an irreversible capacity loss of approximately 50 mAh·g<sup>-1</sup> was detected in the initial cycle, after the second cycle, the charge/discharge behavior stabilized, and even after 80 cycles, a discharge capacity of 105 mAh·g<sup>-1</sup> was maintained. The capacity value indicates that x in  $Li_{2-x}NbHO_2$  reaches up to

Journal Name COMMUNICATION

approximately 0.55 based on  $Nb^{4+}/Nb^{3+}$  redox reaction during charge/discharge. This result means that  $Li_2NbHO_2$  has sufficient  $Li^+$  intercalation ability, and it may be possible to achieve higher voltage and capacity by partial substitution of Nb with 3d transition-metals such as Ni, Co, Mn, and Fe, which are effective as redox species for cathode materials.

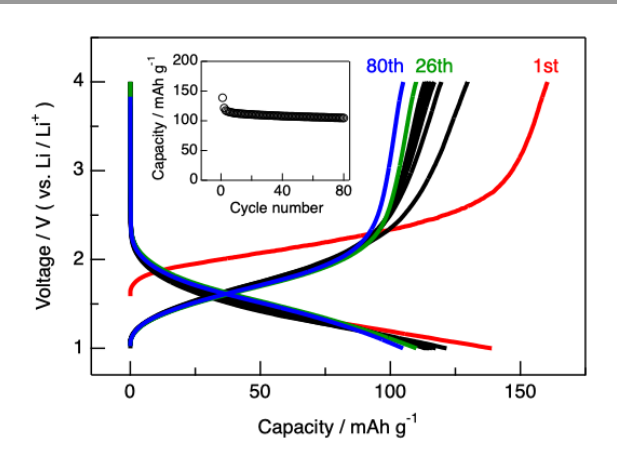


Figure 3 Charge/discharge curves for  $\text{Li}_2\text{NbHO}_2$  electrode between 1.0 and 4.0 V (vs.  $\text{Li/Li}^{\circ}$ ) at a rate of C/10(= 38.3 mA·g<sup>-1</sup>) at 25 °C. Inset: discharge capacity retention upon cycling up to 80 cycles. Li metal foil was used as the counter electrode, and 1M LiPF, dissolved in a 1:1v/v mixture of ethylene carbonate/diethyl carbonate (EC/DEC; Kishida Chemical) was employed as the electrolyte. Working electrode was formulated with 83wt% active materials, 10wt% acetylene black, and 7wt% polytetrafluoroethylene (PTFE). The obtained electrode sheets were dried under vacuum.

In summary, we successfully synthesized  $\text{Li}_2\text{Nb}^{\text{II}}\text{HO}_2$ , the first transition-metal (TM) oxyhydride with a rock-salt-type structure, using mechanochemical methods. The discovery of a new compound with one of the most common crystal structures opens up opportunities for further development in solid-state hydride chemistry. Given that there are many examples of synthesizing H<sup>-</sup> conductors that do not contain TM elements using lithium hydride (LiH) as a raw material<sup>4, 5, 23</sup>, direct synthesis involving TM elements with LiH may have the potential to create an even more diverse group of materials. Moreover, the observed Li<sup>+</sup> intercalation ability suggests that H<sup>-</sup> species could function as a new dopant to enhance electrode performance, such as improving electrical conductivity and tuning voltage.

This work was supported by JSPS, KAKENHI (JP24H00390, JP24H02204, JP22H04514, JP24H02205, and JP22K14755), JST, PRESTO (JPMJPR20T2) and FOREST (JPMJFR213H). The synchrotron radiation experiments were performed at BL01B1 of SPring-8 (2023B2008), with the approval of the Japan Synchrotron Radiation Research Institute (JASRI). The neutron experiments were conducted at J-PARC (2019S10 and 2024S10). FT acknowledges grants from the UBE Industries Foundation and the Kato Foundation for Promotion of Science.

### **Data availability**

The authors confirm that the data supporting the findings of this study are available within the article and supplemental information.

### **Conflicts of interest**

There are no conflicts to declare.

#### Notes and references

- Y. Kobayashi, Y. Tang, T. Kageyama, H. Yamashita, N. Masuda, S. Hosokawa and H. Kageyama, J. Am. Chem. Soc., 2017, 139, 18240-18246.
- 2 M. Miyazaki, K. Ogasawara, T. Nakao, M. Sasase, M. Kitano and H. Hosono, *J. Am. Chem. Soc.*, 2022, 144, 6453-6464.
- 3 M. Kitano, J. Kujirai, K. Ogasawara, S. Matsuishi, T. Tada, H. Abe, Y. Niwa and H. Hosono, J. Am. Chem. Soc., 2019, 141, 20344-20353.
- 4 G. Kobayashi, Y. Hinuma, S. Matsuoka, A. Watanabe, M. Iqbal, M. Hirayama, M. Yonemura, T. Kamiyama, I. Tanaka and R. Kanno, *Science*, 2016, 351, 1314-1317.
- 5 F. Takeiri, A. Watanabe, K. Okamoto, D. Bresser, S. Lyonnard, B. Frick, A. Ali, Y. Imai, M. Nishikawa, M. Yonemura, T. Saito, K. Ikeda, T. Otomo, T. Kamiyama, R. Kanno and G. Kobayashi, Nat. Mater., 2022, 21, 325-330.
- 6 K. Fukui, S. Iimura, T. Tada, S. Fujitsu, M. Sasase, H. Tamatsukuri, T. Honda, K. Ikeda, T. Otomo and H. Hosono, Nat. Commun., 2019, 10, 2578.
- 7 T. Yamamoto, D. Zeng, T. Kawakami, V. Arcisauskaite, K. Yata, M. A. Patino, N. Izumo, J. E. McGrady, H. Kageyama and M. A. Hayward, *Nat. Commun.*, 2017, 8, 1217.
- Y. Iwazaki, T. Suzuki and S. Tsuneyuki, J. Appl. Phys., 2010, 108, 083705.
- 9 T. Sakaguchi, Y. Kobayashi, T. Yajima, M. Ohkura, C. Tassel, F. Takeiri, S. Mitsuoka, H. Ohkubo, T. Yamamoto, J. Kim, N. Tsuji, A. Fujihara, Y. Matsushita, J. Hester, M. Avdeev, K. Ohoyama and H. Kageyama, *Inorg. Chem.*, 2012, 51, 11371-11376.
- 10 C. Tassel, Y. Goto, Y. Kuno, J. Hester, M. Green, Y. Kobayashi and H. Kageyama, *Angew. Chem.*, 2014, 53, 10377-10380.
- 11 T. Yamamoto, K. Shitara, S. Kitagawa, A. Kuwabara, M. Kuroe, K. Ishida, M. Ochi, K. Kuroki, K. Fujii, M. Yashima, C. M. Brown, H. Takatsu, C. Tassel and H. Kageyama, *Chem. Mater.*, 2018, 30, 1566-1574.
- 12 K. Higashi, M. Ochi, Y. Nambu, T. Yamamoto, T. Murakami, N. Yamashina, C. Tassel, Y. Matsumoto, H. Takatsu, C. M. Brown and H. Kageyama, *Inorg. Chem.*, 2021, 60, 11957-11963.
- 13 M. A. Hayward, E. J. Cussen, J. B. Claridge, M. Bieringer, M. J. Rosseinsky, C. J. Kiely, S. J. Blundell, I. M. Marshall and F. L. Pratt, *Science*, 2002, 295, 1882-1884.
- 14 F. Denis Romero, A. Leach, J. S. Moller, F. Foronda, S. J. Blundell and M. A. Hayward, Angew. Chem., 2014, 53, 7556-7559.
- 15 R. D. Shannon, Acta Crystallogr. Sect. A, 1976, 32, 751-767.
- 16 T. Uchimura, F. Takeiri, K. Okamoto, T. Saito, T. Kamiyama and G. Kobayashi, *J. Mater. Chem. A*, 2021, 9, 20371-20374.
- 17 R. Oishi, M. Yonemura, Y. Nishimaki, S. Torii, A. Hoshikawa, T. Ishigaki, T. Morishima, K. Mori and T. Kamiyama, *Nucl. Instrum. Methods Phys. Res. A*, 2009, 600, 94-96.
- 18 K. Momma and F. Izumi, *J. Appl. Crystallogr.*, 2011, 44, 1272-1276.
- 19 C. Suryanarayana, *Prog. Mater Sci.*, 2001, 46, 1-184.
- 20 N. Yabuuchi, M. Takeuchi, M. Nakayama, H. Shiiba, M. Ogawa, K. Nakayama, T. Ohta, D. Endo, T. Ozaki, T. Inamasu, K. Sato and S. Komaba, *Proc Natl Acad Sci*, 2015, 112, 7650-7655.
- 21 J. Lee, D. A. Kitchaev, D.-H. Kwon, C.-W. Lee, J. K. Papp, Y.-S. Liu, Z. Lun, R. J. Clément, T. Shi, B. D. McCloskey, J. Guo, M. Balasubramanian and G. Ceder, *Nature*, 2018, 556, 185-190.
- 22 X. Lan, X. Liu, T. Meng, S. Yang, Y. Shen and X. Hu, Small Methods, 2023, 7, 2201290.
- 23 T. Hirose, T. Mishina, N. Matsui, K. Suzuki, T. Saito, T. Kamiyama, M. Hirayama and R. Kanno, *ACS Appl. Energy Mater.*, 2022, 5, 2968-2974.

ChemComm Page 4 of 4

The data supporting the findings of this study are available from the authors upon request.